Multiwalled Carbon Nanotube Nucleated Crystallization Behavior of Biodegradable Poly(butylene succinate) Nanocomposites

K. P. Pramoda,[1] N. T. T. Linh,[1] Chao Zhang,[2] Tianxi Liu[2]

[1]*Institute of Materials Research and Engineering, Agency for Science, Technology, and Research, 3 Research Link, Singapore 117602*
[2]*Key Laboratory of Molecular Engineering of Polymers (Ministry of Education), Department of Macromolecular Science, Fudan University, Shanghai 200433, People's Republic of China*

Received 29 May 2008; accepted 1 September 2008
DOI 10.1002/app.29349
Published online 5 December 2008 in Wiley InterScience (www.interscience.wiley.com).

ABSTRACT: Poly(butylene succinate) (PBS) nanocomposites with multiwalled carbon nanotubes (MWNTs) prepared by melt compounding were studied for the effect of MWNT dispersion on the modulus and crystallization kinetics. The nucleating effect of the addition of 0.1 wt % MWNT to PBS was clearly demonstrated. Differential scanning calorimetry nonisothermal crystallization studies showed a clear decrease in the half-time of crystallization with increasing MWNT content in PBS/MWNT nanocomposites. It was observed with the Ozawa method that the Ozawa parameter values for the nanocomposites were lower than those for neat PBS, and this indicated that the crystal morphology was different. The storage modulus of the nanocomposites increased about 23% with the addition of only 0.1% MWNT in comparison with neat PBS, whereas the glass-transition temperature was unaltered. © 2008 Wiley Periodicals, Inc. J Appl Polym Sci 111: 2938–2945, 2009

Key words: crystallization; nanocomposites

INTRODUCTION

The preparation and characterization of polymer nanocomposite materials have aroused a great deal of interest among researchers over the past few years.[1,2] This is mainly due to their enhanced properties, including their mechanical strength, barrier behavior, thermal stability, and heat deflection temperature. This property enhancement is mainly due to the high aspect ratio and low density of the nanoparticle reinforcement in the polymer matrix. Common nanoreinforcements are organoclay, carbon nanotubes (CNTs), polyhedral oligomeric silsesquioxanes, SiO_2, and mica.[1–4] Among them, CNTs have recently become more attractive because of their electrical conductivity, electromagnetic interference shielding, and mechanical properties.[5–7]

Poly(butylene succinate) (PBS) is a biodegradable aliphatic polyester and is semicrystalline in nature. It has a wide range of engineering applications because of its attractive combination of good processability and mechanical properties.[8,9] Recently, both conducting polymer–clay nanocomposites and conducting polymer–CNT composites have been widely studied to produce large-scale enhancements of the physical, mechanical, optical, and conducting properties.[10–17] Chen and Yoon[12] showed that the crystallization of PBS was accelerated as a result of the incorporation of an organoclay, and it was more pronounced with an epoxy-functionalized organoclay because of the enhanced nucleation effect of the more finely dispersed clay layers. Another study of a PBS/3 wt % multiwalled carbon nanotube (MWNT) nanocomposite[13] showed an enhancement of the mechanical properties and conductivity of the composites. Ray et al.[15] studied PBS/organoclay nanocomposites and showed that there was a drastic improvement in the modulus and thermal stability of the composite samples in comparison with neat PBS.

The study of the nonisothermal crystallization of nanocomposites is of technological importance as most composites and polymer blends are processed under nonisothermal conditions. Structural properties such as the crystallinity and density and mechanical properties are also related to crystallization conditions. Studies of polymer/MWNT composites are expanding because of commercial research and

Correspondence to: K. P. Pramoda (pramoda-kp@imre.a-star.edu.sg).

Contract grant sponsor: Opening Project of the Key Laboratory of Biomedical Polymers of the Ministry of Education, Wuhan University (to T. X. L.); contract grant number: 20070503.

development interest as they can be used as advanced structural materials on account of their attractive mechanical properties and because they might possibly replace aluminum.[10–17] Hence, an understanding of optimum fabrication conditions, such as processing, interfacial strength, and crystallization behavior, is urgently needed and requires in-depth investigation.

In this article, we report the morphology and crystallization behavior of PBS/MWNT nanocomposites. The MWNT-initiated polymer crystallization behavior was studied. The main objectives of the work are (1) to study in detail the nonisothermal crystallization kinetics of PBS/MWNT nanocomposites and compare the results to those of neat PBS and (2) to describe the effect of MWNT on the crystal morphology and mechanical properties of the PBS matrix.

EXPERIMENTAL

Materials and PBS/CNT nanocomposites

PBS used in this study was purchased from Sigma–Aldrich (China). The MWNTs were prepared by the catalytic chemical vapor deposition of methane on Co–Mo/MgO catalysts. The as-prepared MWNTs were purified by an acid treatment, which has been described in detail elsewhere.[18] PBS composites containing different amounts (0–2 wt %) of MWNTs were prepared via a melt-compounding method with a Brabender twin-screw mixer at 130°C for 10 min with a screw speed of 100 rpm. Film samples (with a thickness of 0.5 mm) were prepared by compression molding in a press at a temperature of 130°C and a pressure of 15 MPa, followed by rapid quenching in an ice–water bath. Note that the melting temperature (T_m) of PBS is about 115°C as estimated by differential scanning calorimetry (DSC) measurements.

Characterization

The crystallization and melting behavior of neat PBS and its nanocomposites with different concentrations of MWNTs was studied by DSC with a TA DSC 2980 (New Castle, DE) that had been calibrated with an indium standard under a nitrogen flow rate of 20 mL/min. Cooling and heating rates (β) of 2.5, 5, 10, and 20°C/min were used. The samples were first heated to 140°C and then cooled to 30°C. The morphology was examined with a polarized optical microscope (Nikon, New York, NY) coupled to a Linkam FP-90 hot stage. The images were captured with a digital camera.

RESULTS AND DISCUSSION

Structure and morphology of the PBS/CNT nanocomposites

X-ray diffraction (XRD) analysis was performed at room temperature, and the patterns are shown in Figure 1(a). The XRD patterns of the neat PBS and its MWNT nanocomposite samples are quite similar. This indicates that the samples had the same crystal structure, an α-form of the PBS crystal. The main characteristic diffraction peaks observed at 2θ values of 19.7, 21.9, and 22.8° are assigned to (020), (021),

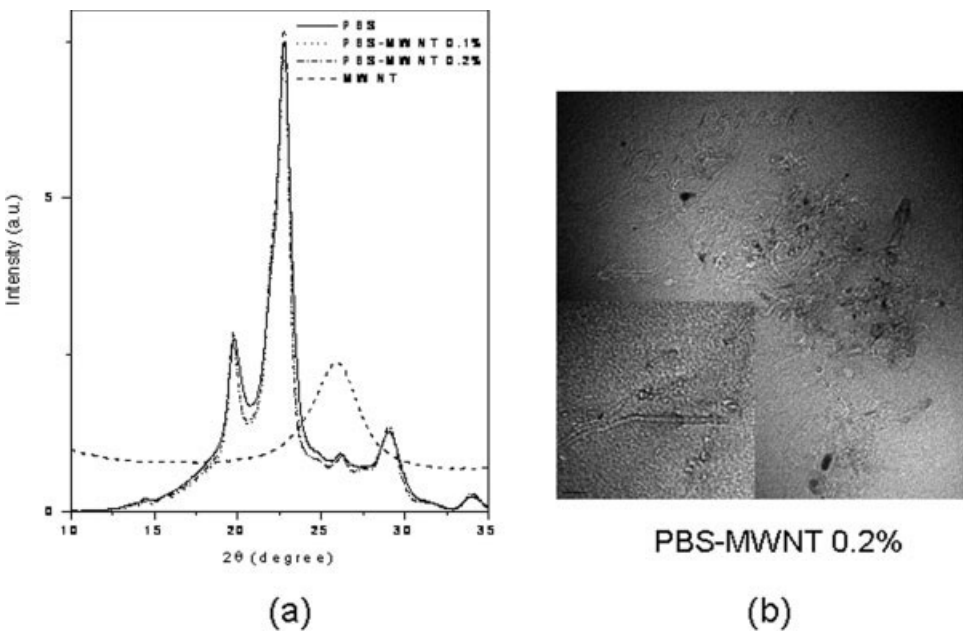

Figure 1 (a) XRD patterns of neat PBS and MWNT nanocomposite samples and (b) transmission electron micrograph of PBS/MWNT 0.2%.

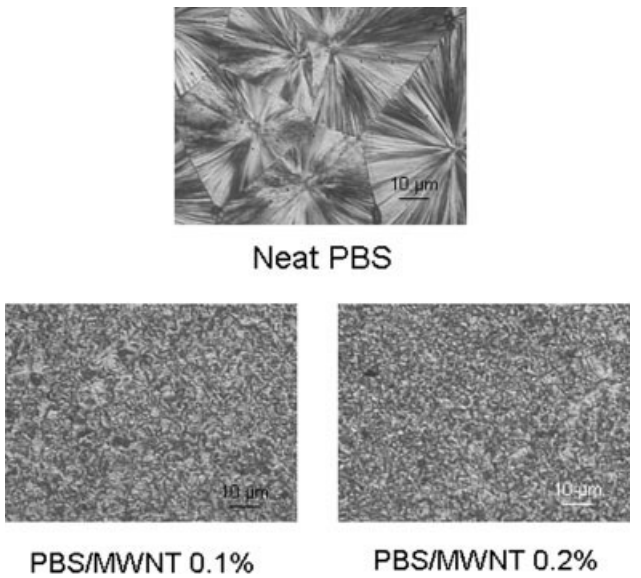

Figure 2 Polarized optical microscopy morphology of neat PBS and its nanocomposites.

and (110) planes of the α-form PBS crystal.[9] Figure 1(b) presents a transmission electron micrograph of a PBS nanocomposite sample with 0.2 wt % MWNT. It indicates the dispersion of MWNT in the PBS matrix, and the inset shows a high-magnification image of the micrograph.

The crystallization behavior, as observed with optical microscopy, is shown in Figure 2. It shows classical Maltese cross patterns in PBS spherulites. The well-defined spherulites are much larger for neat PBS than those for PBS/MWNT nanocomposites, and this indicates that the MWNTs act as nucleating sites for PBS crystallization. However, apart from being small spherulites, they are also imperfect and grow rapidly, being nucleated by the addition of MWNTs and impinged by the surrounding spherulites, which restrict further growth of the spherulites. The neat PBS showed crystallites with a size of about 30 μm, whereas the PBS/MWNT composite showed crystallites only about 1–2 μm in size.

Crystallization and melting behavior

Crystallinity plays an important role in the physical properties and biodegradability of biodegradable polymers. Moreover, the crystalline structure and morphology of a semicrystalline polymer are also influenced greatly by its thermal history. Figure 3(a,b) shows the DSC heating and cooling thermograms for neat PBS and its nanocomposites measured at a heating (cooling) rate of 10°C/min. Although the exothermic peaks represent the crystallization process, the endothermic peaks correspond to the melting of PBS and its MWNT nanocomposite samples. The crystallization peak temperature (T_p) and T_m of neat PBS and its nanocomposites were thus obtained and are listed in Table I. T_p of PBS (83°C) increases with the incorporation of MWNTs (95°C), and this implies that the crystallization of PBS is faster in the presence of MWNTs. It is believed that the addition of MWNTs induces the crystallization of PBS. However, in comparison with neat PBS, T_m (∼ 114°C) is not much affected either by the addition of MWNTs or different heating rates, probably because of their small size and the low component of the MWNTs in the nanocomposites. In addition, both the melting and crystallization peaks in the PBS/MWNT nanocomposites are narrower than those in neat PBS. This would suggest a

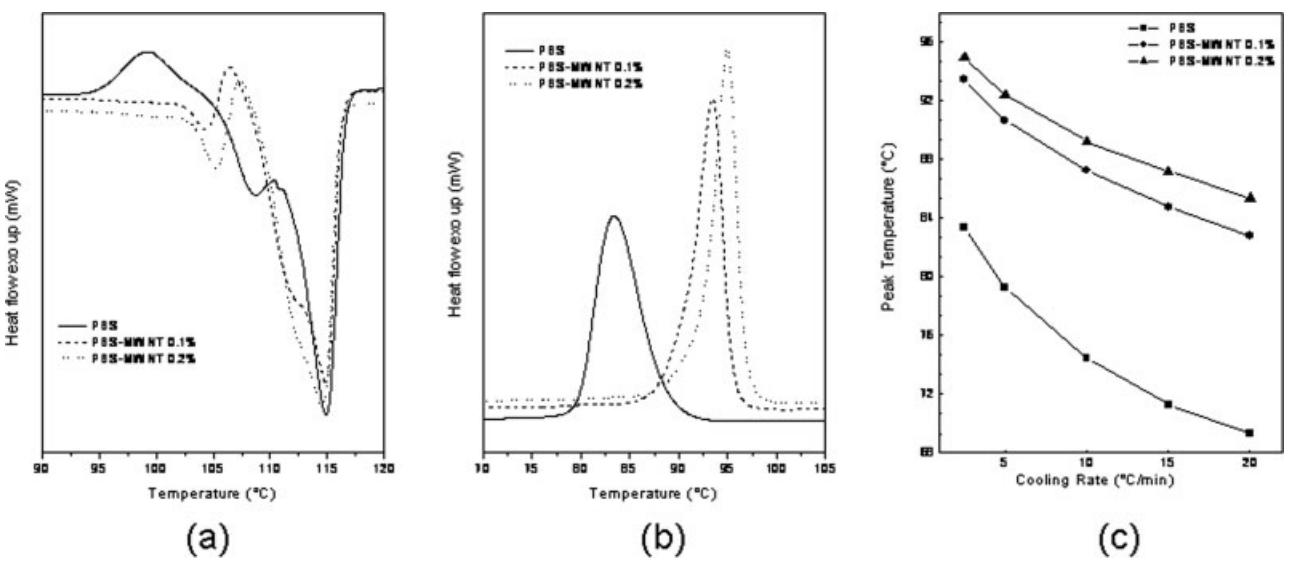

Figure 3 (a) DSC heating thermograms, (b) DSC cooling thermograms, and (c) T_p values for neat PBS and its nanocomposites.

TABLE I
Melting and Crystallization Temperatures and Crystallinity Values for PBS and Its MWNT Nanocomposites

Sample	β (°C/min)	T_m (°C)	T_{on} (°C)	T_p (°C)	ΔH_m (J/g)	X_t (%)	$t_{1/2}$ (min)
PBS	2.5	115	88.5	83.4	91.2	43.4	4
	5	114.5	84.7	79.3	94.1	44.8	2.5
	10	114.4	80.4	74.5	91.5	43.6	1.3
	15	114	77.6	71.3	89	42.4	1
	20	115	75.7	69.4	84.5	40.2	0.7
PBS/MWNT 0.1%	2.5	114.9	95.4	93.5	69.4	33	2.7
	5	114.4	93	90.7	67.7	32	1.7
	10	114.3	90	87.3	65.2	31	0.9
	15	114.4	88	84.8	62.8	29.9	0.7
	20	114.3	86.5	82.8	61.5	29.3	0.5
PBS/MWNT 0.2%	2.5	114.5	96.7	95	72	34.3	2.8
	5	114.1	94.4	92.4	69.4	33	1.4
	10	113.8	91.6	89.2	68.3	32.5	0.8
	15	113.8	89.8	87.2	66.2	31.5	0.6
	20	114.1	88.5	85.4	66.2	31.5	0.5

narrower crystallite size distribution in the PBS/MWNT nanocomposites versus neat PBS.

As shown in Table I, an increase in T_p of PBS can be observed due to the presence of MWNTs. It is clearly shown that the incorporation of MWNTs into PBS results in an increase in the crystallization temperature. The crystallinity percentages for neat PBS and its MWNT nanocomposites were determined with the following equation:

$$\text{Crystallinity}(\%) = \frac{\Delta H_m}{\Delta H_m^0} \times 100\% \quad (1)$$

where ΔH_m and ΔH_m^0 are the melting enthalpies of the crystalline sample and the standard melting enthalpy of a perfect PBS crystal (210 J/g),[8] respectively. Here we assume the same perfect crystallization enthalpies for PBS and PBS/MWNT samples and evaluate the crystallinity of both PBS and PBS/MWNT samples according to eq. (1). As shown in Table I, the crystallinity of the neat PBS decreases from 43 to 33% in the presence of MWNTs.

The values of T_p for PBS and PBS/MWNT samples at different cooling rates are shown in Figure 3(c). T_p decreases with an increasing cooling rate. The incorporation of MWNTs into the PBS matrix results in an increase in T_p of about 10°C, and this indicates that the presence of MWNTs induces the crystallization of PBS chains. The trend of the dependence of T_p on the cooling rate for PBS/MWNT systems is similar to that obtained for neat PBS. This observation is consistent with studies in the literature[11–13] on the crystallization behavior of PBS with the addition of an organoclay. Figure 3(c) shows that at a given cooling rate, T_p increases with the MWNT content increasing, and this indicates that the crystallization rate increases with MWNTs. As expected, the value of the half-time of crystallization ($t_{1/2}$) decreases with an increasing cooling rate for both PBS and PBS/MWNT composites. The values of $t_{1/2}$ for the PBS/MWNT composites are smaller than those for neat PBS, and this indicates that the presence of MWNTs accelerates the overall crystallization of PBS. The effect of MWNT addition on PBS crystallization is probably twofold: the presence of MWNTs provides heterogeneous nucleation sites for PBS crystallization and hinders the formation of large crystals.

Nonisothermal crystallization kinetics

The relative degree of crystallinity (X_t) as a function of the crystallization temperature for the neat PBS and PBS/MWNT composites at various cooling rates is plotted in Figure 4. T_p of PBS and PBS/MWNT composites decreases with increasing cooling rates. All curves in Figure 4(a–c) show a reverse sigmoidal shape, suggesting that the crystal nucleation takes place freely from the melt and slows down during the crystal growth. To describe the evolution of crystallinity in a nonisothermal crystallization process, a number of kinetic models are available in the literature. In this report, we have used mainly the Ozawa[19] and Mo[20] models to describe the nonisothermal crystallization behavior, the Kissinger,[21] Takhor,[22] and Augis–Bennett[23] methods for the activation energy estimation, and the Dobreva model[24] for the nucleation determination.

Figure 5 shows the nonisothermal crystallization kinetics of PBS and its MWNT nanocomposites with the Ozawa method. Data analysis was carried out from plots of $\ln[-\ln(1 - X_t)]$ versus $\ln \beta$ within the crystallization temperature range of 64–86°C for neat PBS and within the crystallization temperature range of 74–94°C for the nanocomposites. Qualitatively, the Ozawa method is satisfactory for describing the

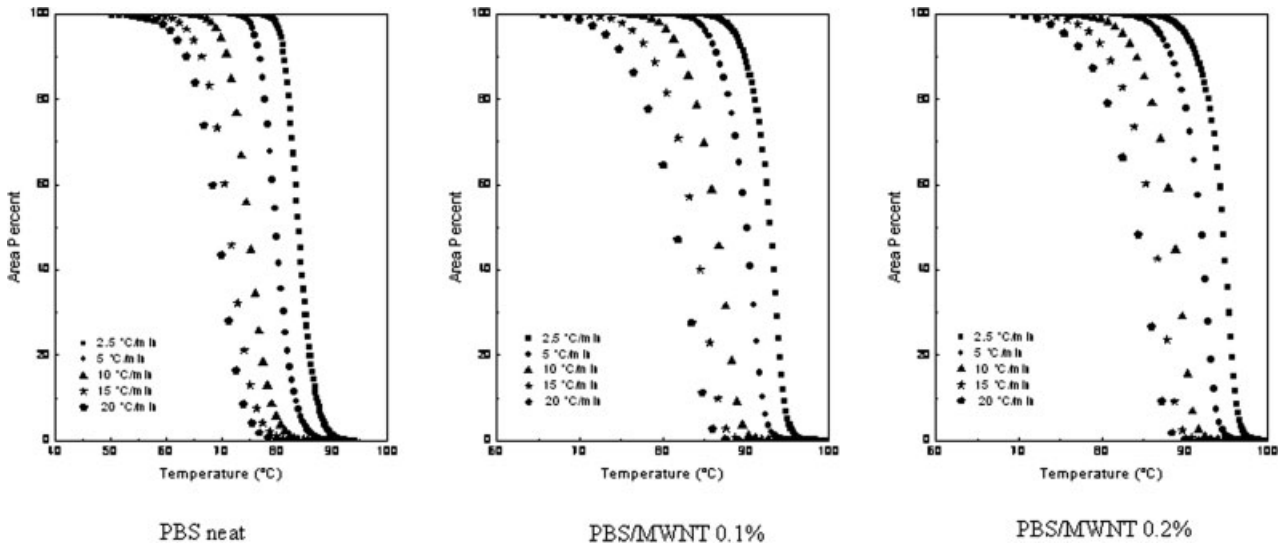

Figure 4 Variation of X_t with the temperature for nonisothermal crystallization.

nonisothermal crystallization of PBS and PBS/MWNT nanocomposites, as shown in Figure 5. X_t strongly depends on the cooling rate at the initial stage of crystallization but is affected slightly by the cooling rate at the end of the crystallization process. The kinetic parameters [i.e., Ozawa exponent m and kinetic parameter $\phi(T)$], analyzed by the Ozawa method, are summarized in Table II. The average values of m are 3.1 for PBS and 2.8 and 2.3 for its nanocomposites containing 0.1 and 0.2 wt % MWNTs, respectively. The value of $\phi(T)$ for neat PBS decreases with increasing temperature, except at an early stage of crystallization, and this suggests that the crystallization is a nucleation-controlled process. However, in the PBS/MWNT systems, it is interesting to note that $\phi(T)$ increases with an increase in temperature at the initial stage of crystallization, whereas a decrease with increasing temperature can be observed at the later stage of crystallization. It implies that the crystallization is hindered by the presence of MWNTs, and the overall rate of the crystallization process will thus be reduced.

Mo's model is a combination of the Ozawa and Avrami equations. The importance of this method is that it correlates cooling rate β to the crystallization time t or temperature T and the morphology for a given degree of crystallinity as follows:

$$\ln \beta = \ln F(T) - b \ln t \tag{2}$$

where $F(T) = [K(T)/Z_t]^{1/m}$ refers to the value of the cooling rate chosen at the unit of crystallization time when the system has a certain degree of crystallinity

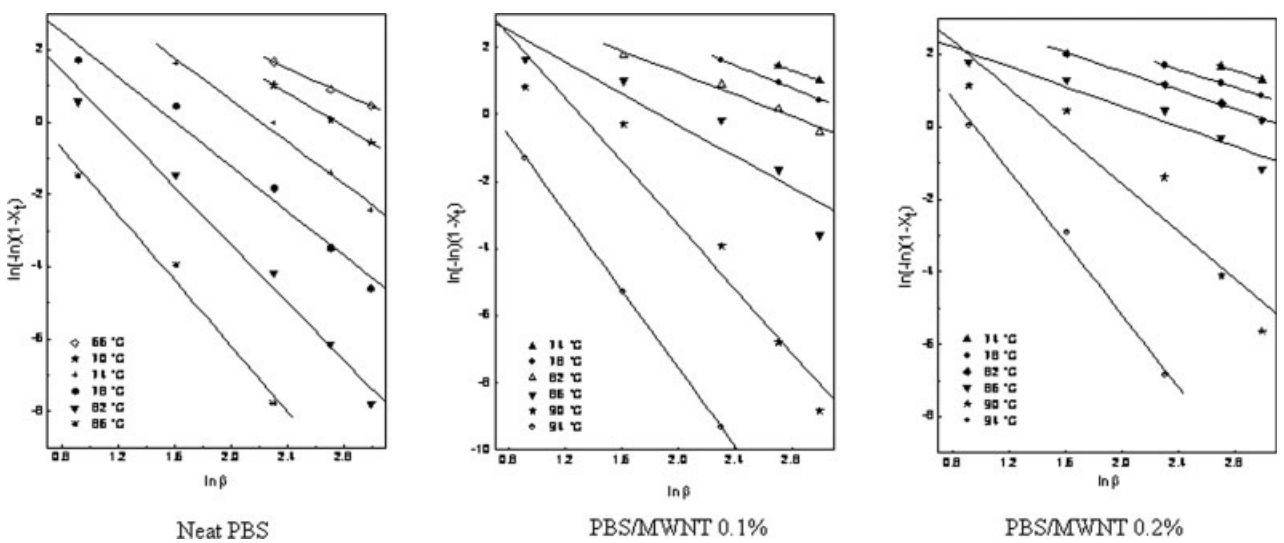

Figure 5 Ozawa plots of $\ln[-\ln(1 - X_t)]$ versus ln β for the crystallization of neat PBS and PBS/MWNT samples.

TABLE II
Nonisothermal Crystallization Kinetics of PBS and Its Nanocomposites Analyzed by Ozawa, Kissinger, Takhor, and Augis–Bennett Methods

Temperature (°C)	m	$\phi(T)$	Activation energy (kJ/mol) Kissinger	Takhor	Augis–Bennett
PBS			175	148	132
66	1.77	5.72			
70	2.31	6.35			
74	2.89	6.41			
78	3.09	4.96			
82	3.99	4.62			
86	4.55	2.89			
PBS/MWNT 0.1%			235	211	146
74	1.53	5.60			
78	1.65	5.41			
82	1.62	4.48			
86	2.27	4.26			
90	4.72	6.15			
94	5.79	4.02			
PBS/MWNT 0.2%			263	239	178
74	1.29	5.17			
78	1.24	4.55			
82	1.29	4.13			
86	1.38	3.32			
90	3.27	4.97			
94	4.97	4.75			

and b is the ratio of the Avrami exponent (n) to m, that is, $b = n/m$. At a given degree of crystallinity, the plot of ln β against ln t provides a straight line with an intercept of ln[$F(T)$] and a slope of $-b$ (the figure is not shown here for brevity). The $F(T)$ and b values obtained from the straight lines are listed in Table III. The $F(T)$ values increase with X_t. $F(T)$ and b values for the nanocomposites are lower than those for neat PBS, indicating that the crystallization process in the nanocomposites is faster than that in the neat PBS. This result confirms the effect of MWNTs on the crystallization as nucleating agents, as discussed earlier.

Dobreva and Gutzow[24] proposed a simple method for the determination of the nucleating activity of a foreign body in a polymer melt. The nucleation activity (ψ) is a factor by which the three-dimensional nucleation process decreases with the addition of a filler. If the filler is extremely active for the nucleation, ψ approaches 0, whereas for an inert filler, it approaches 1. For homogeneous nucleation near T_m, cooling rate β is related to T_p:

$$\log \beta = A - \frac{B}{2.3\Delta T_p^2} \tag{3}$$

For heterogeneous nucleation, it becomes

$$\log \beta = A - \frac{B^*}{2.3\Delta T_p^2} \tag{4}$$

$$\psi = \frac{B^*}{B} \tag{5}$$

where A is a constant and ΔT_p is the degree of supercooling (i.e., $\Delta T_p = T_m - T_p$). B is a parameter that can be calculated from the following equation:

$$B = \frac{\omega\sigma^3 V_m^2}{3nkT_m\Delta S_m^2 n} \tag{6}$$

where ω is a geometrical factor, σ is the specific energy, V_m is the molar volume of the crystallizing substance, ΔS_m is the entropy of melting, and k is the Boltzmann constant. Therefore, ψ can be determined simply from the ratio of the slope of the plot of log β versus $1/\Delta T_p^2$ in the presence of the nucleation agent or in the absence of the nucleation agent. Figure 6 shows plots of log β versus $1/\Delta T_p^2$ for neat PBS and PBS/MWNT composites. The ψ values of PBS/MWNT composites containing 0.1 and 0.2 wt % MWNT were calculated to be 0.5 and 0.4, respectively. As mentioned previously, the presence of a nanofiller, which serves as a nucleating agent and affects the

TABLE III
Kinetic Parameters Based on Mo's Method

Sample	Kinetic parameters	X_t (%) 20	40	60	80
PBS	$F(T)$	2.37	2.56	2.70	2.87
	b	1.19	1.19	1.2	1.24
PBS/MWNT 0.1%	$F(T)$	1.90	2.07	2.22	2.49
	b	1.11	1.16	1.21	1.25
PBS/MWNT 0.2%	$F(T)$	1.83	1.98	2.15	2.40
	b	1.06	1.11	1.16	1.21

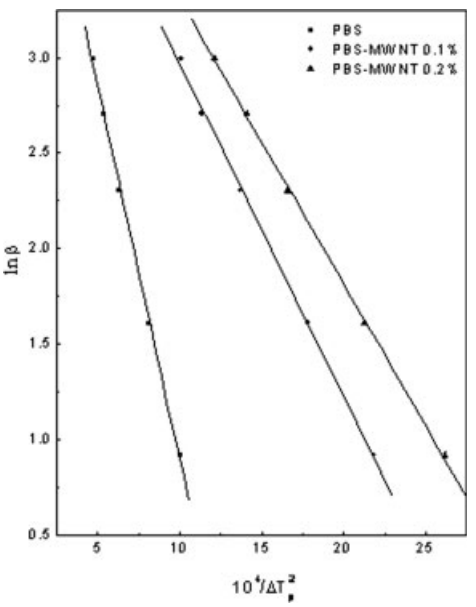

Figure 6 Plots of log β versus $1/\Delta T_p^2$ for neat PBS and PBS/MWNT nanocomposites.

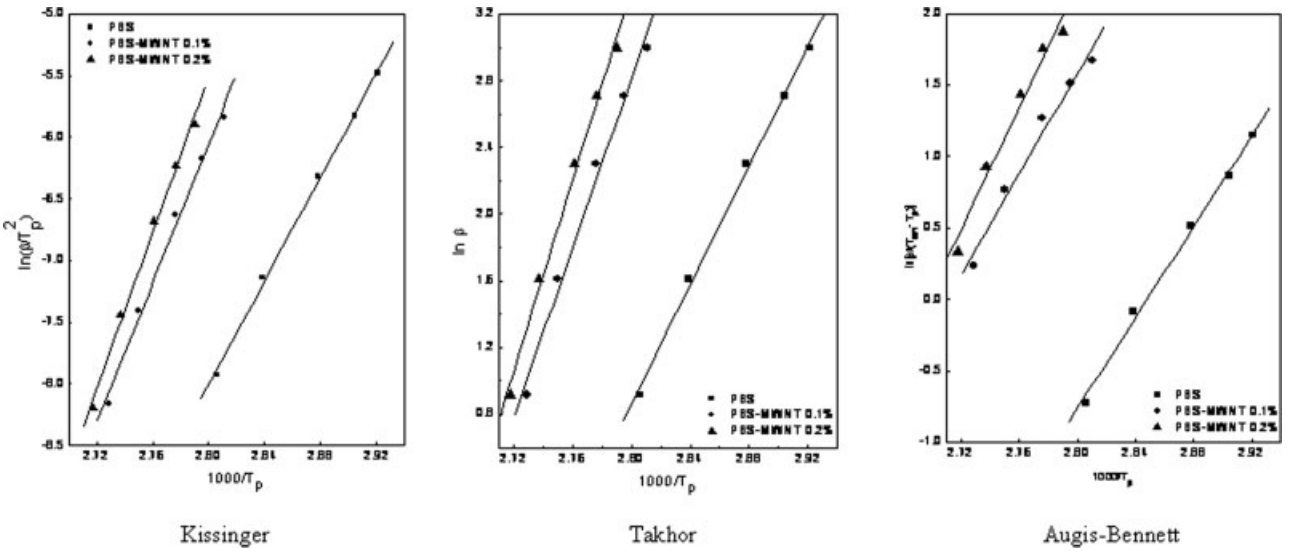

Figure 7 Calculated activation energy for nonisothermal crystallization based on the Kissinger, Takhor, and Augis–Bennett methods.

molecular mobility, also affects the crystallization behavior and crystalline structures of the material.

The activation energy for nonisothermal crystallization (ΔE_a) can be calculated on the basis of the variation in the onset crystallization temperature (T_{on}), T_p, and β through the plotting of the following equations with different methods. According to Kissinger, the apparent activation energy is described by the following equation:

$$\frac{d[\ln(\beta/T_p^2)]}{d(1/T_p)} = -\frac{\Delta E_a}{R} \tag{7}$$

where R is the universal gas constant.

Based on the Augis–Bennett method, the activation energy is given by the following equation:

$$\frac{d[\ln(\beta/(T_{on} - T_p)]}{d(1/T_p)} = -\frac{\Delta E_a}{R} \tag{8}$$

According to the Takhor method

$$\frac{d(\ln \beta)}{d(1/T_p)} = -\frac{\Delta E_a}{R} \tag{9}$$

Figure 7(a–c) shows linear plots of $\ln(\beta/T_p^2)$, $\ln[\beta/(T_{on} - T_p)]$, and $\ln \beta$ against $1/T_p$, respectively, for both PBS and its MWNT nanocomposites. The activation energies were determined from the slopes ($-\Delta E_a/R$) of the linear regressions, and the results are tabulated in Table II. The activation energy for neat PBS is 175 kJ/mol, whereas that of the nanocomposites is 235 or 263 kJ/mol when 0.1 or 0.2 wt % MWNT is incorporated, respectively, according to the Kissinger method. Although lower values are seen with the Takhor and Augis–Bennett methods, a similar trend can be seen for the three approaches: neat PBS has the lowest value in comparison with its MWNT nanocomposites.

Usually, the crystallization activation energy indicates the crystallization ability of polymers. The higher the activation energy is, the lower the crystallization ability is. The overall crystallization process is the combination of nucleation and growth. Polymer chains are highly entangled in the melt state, and during crystallization, the polymer chains must overcome certain energy barriers to diffuse and attach onto the growing front of a crystal. However, in the nanocomposites, MWNTs act as an embryonic crystal or nucleus for the heterogeneous nucleation of polymer chains. Hence, the nucleation density will be higher for higher MWNT content samples. In addition, MWNTs can be visualized as long stiff chains of carbon atoms and possibly act as a constraint on the polymer chain mobility, especially when they have good interactions with polymer chains. Therefore, the presence of MWNTs here probably plays two different or competing roles for the crystallization of PBS, that is, promoting the nucleation process by acting as a heterogeneous nucleating agent and, at the same time, hindering the crystal growth process by imposing the constraints upon the surrounding polymer chains.

CONCLUSIONS

PBS/MWNT nanocomposites were prepared by melt compounding. The storage modulus was found to increase by about 23% with an MWNT content of only 0.1 wt %. The nucleating effect of the addition of MWNTs to PBS was clearly demonstrated. The nonisothermal crystallization studies showed a clear decrease in $t_{1/2}$ with increasing MWNT content in

PBS/MWNT nanocomposites. From the Ozawa method, lower m values were observed for the nanocomposites in comparison with neat PBS, indicating that the crystal morphology was changed. The presence of MWNTs increased the activation energy of the nanocomposites and also contributed to ψ.

Two of the authors (P.K.P. and N.T.T.L.) gratefully acknowledge the continued support of the research work presented in this article by the Institute of Materials Research and Engineering of the Agency for Science, Technology, and Research.

References

1. Pinnavaia, T. J.; Beall, G. W. Polymer–Clay Nanocomposites; Wiley: New York, 2001.
2. Polymer Nanocomposites: Synthesis, Characterization and Modeling; Krishnamoorti, R.; Richard, A. V., Eds.; American Chemical Society: Washington, DC, 2002.
3. Ajayan, P. M.; Schadler, L. S.; Braun, P. V. Nanocomposite Science and Technology; Wiley-VCH: Weinheim, 2003.
4. Baughman, R. H.; Zakhidov, A. A.; de Heer, W. A. Science 2002, 297, 787.
5. Terrones, M. Annu Rev Mater Res 2003, 33, 419.
6. Li, H. H.; Zhang, X.; Kuang, X.; Wang, J. C.; Wang, D. J.; Li, L.; Yan, S. K. Macromolecules 2004, 37, 2847.
7. Ajayan, P. M.; Schadler, L. S.; Giannaris, C.; Rubio, A. Adv Mater 2000, 12, 750.
8. Papageorgiou, G. Z.; Achilias, D. S.; Bikiaris, D. N. Macromol Chem Phys 2007, 208, 1250.
9. Yoo, E. S.; Im, S. S. J Polym Sci Part B: Polym Phys 1999, 37, 1357.
10. Kodjie, S. C.; Li, L.; Li, B.; Cai, W.; Li, C. Y.; Keating, M. J Macromol Sci Phys 2006, 45, 231.
11. Ray, S. S.; Bousmina, M. Macromol Chem Phys 2006, 207, 1207.
12. Chen, G. X.; Yoon, J. S. J Polym Sci Part B: Polym Phys 2005, 43, 817.
13. Chen, G. X.; Kim, H. S.; Yoon, J. S. Polym Int 2007, 56, 1159.
14. Assouline, E.; Lustiger, A.; Barber, A. H.; Cooper, C. A.; Klein, E.; Wachtel, E.; Wagner, H. D. J Polym Sci Part B: Polym Phys 2003, 41, 520.
15. Ray, S. S.; Vaudreuil, S.; Maazouz, A.; Bousmina, M. J Nanosci Nanotechnol 2006, 6, 2191.
16. Ray, S. S.; Okamoto, K.; Okamoto, M. J Appl Polym Sci 2006, 102, 777.
17. Li, L.; Li, C. Y.; Ni, C.; Rong, L.; Hsiao, B. S. Polymer 2007, 48, 3452.
18. Liu, T. X.; Phang, I. Y.; Shen, L.; Chow, S. Y.; Zhang, W. D. Macromolecules 2004, 37, 7214.
19. Ozawa, T. Polymer 1971, 12, 150.
20. Liu, T. X.; Mo, Z. S.; Wang, S. E.; Zhang, H. F. Polym Eng Sci 1997, 37, 568.
21. Kissinger, H. E. J Res Natl Bur Stand U S A 1956, 57, 217.
22. Takhor, R. L. Advances in Nucleation and Crystallization of Glasses; American Chemical Society: Columbus, OH, 1971; p 166.
23. Augis, J. A.; Bennett, J. E. J Therm Anal 1978, 13, 283.
24. Dobreva, A.; Gutzow, I. J Non-Cryst Solids 1993, 162, 1.